Progress in Fractional Differentiation and Applications
An International Journal

http://dx.doi.org/10.18576/pfda/110202

Atangana Baleanu Caputo Fractional Order Modeling and Analysis for the Transmission of Coffee Berry Disease

Abayneh Kebede Fantaye[1,*] *and Kokobe Teferedegn Ergete*[2], *Faisal Alshowaikh*[3], *Mohamed Hafez*[4], *Betty Wan Niu Voon*[5], *and Shawkat Alkhazaleh*[6]

[1] Department of Mathematics, College of Natural and Computational Sciences, Debre Tabor University, Debre Tabor, Ethiopia
[2] Department of Biology, College of Natural and Computational Sciences, Hawassa University, Hawassa, Ethiopia
[3] Department of Mathematical Sciences, College of Arts and Science, Ahlia University, 10878. Manama. Kingdom of Bahrain
[4] Faculty of Engineering and Quantity Surviving, INTI International University Colleges, Nilai, Malaysia
[5] Department of Civil Engineering, (COE), Universiti Tenaga Nasional, Kajang, Malaysia
[6] Department of Mathematics, Faculty of Sciences, Jadara University, Jordan

Received: 12 Sep. 2024, Revised: 18 Oct. 2024, Accepted: 20 Nov. 2024
Published online: 1 Apr. 2025

Abstract: Coffee Berry Diseases (CBD) pose significant threats to coffee production worldwide, affecting the livelihoods of millions of farmers and the global coffee market. Fractional calculus provides a powerful framework for describing non-local and memory-dependent phenomena, making it suitable for modeling the long-range interactions inherent in CBD spread. This study aims to formulate and analyze fractional order model for CBD transmission dynamics in the sense of Atangana Baleanu Caputo (ABC). Fixed point theorems were utilized to test the existence and uniqueness of the model's solutions using the Caputo operator. The basic reproduction number was calculated utilizing the next-generation matrix. The model has locally asymptotically stable equilibrium positions (disease-free and endemic). Furthermore, the Lyapunov function was used to conduct a global stability analysis of the equilibrium locations. A numerical simulation of the CBD model was created using the fractional Adam-Bashforth-Moulton approach to validate the analytical findings. Our findings contribute to the development of more accurate predictive models and inform the design of targeted interventions to mitigate the impact of CBD on coffee production systems.

Keywords: Coffee Berry diseases, basic reproduction number, fractional order, numerical simulation.

1 Introduction

Coffee is a cultivar that grows well in the varied eco-physiological conditions of tropical and subtropical highlands and can be grown on agricultural land. After crude oil, it is the most consumed beverage and the second most traded commodity worldwide [1]. Although it is the main source of income for tropical countries, which are often less developed, wealthy countries are the ones that consume it the most [2]. The growth of weeds, pests, and diseases have all hampered coffee output. For example, the coffee berry disease caused by Colletotrichum kahawae substantially hinders the production of Arabica coffee in African countries (CBD) [3]. It is a pathogenic fungus that affects plants [4, 5]. Black depressed wounds on coffee berries are one of the signs of CBD [6]. All phases of fruit and flower development are affected by the disease, but immature berries are especially vulnerable during the 4–16 week expanding phase following flowering [7].
In regions with high levels of precipitation, humidity, and altitude, losses could reach 100% [2, 8]. Biological control, pharmacological treatments, cultural customs, the adoption of resistant cultivars, and other approaches are some of the various ways that CBD can be managed [9]. By way of the wind and rain, CBD is dispersed locally between branches and coffee trees [10]. But insects, birds, and coffee harvesters are frequently used vectors for long- and medium-distance CBD dispersal [11]. with healthy coffee berries after coming into touch with a fungal disease from the environment or coffee berries that have already been infected with CBD were responsible for the spread of the drug [12].

* Corresponding author e-mail: abayk400@gmail.com

© 2025 NSP
Natural Sciences Publishing Cor.

The dynamics of plant disease have been modeled mathematically and examined by different authors ([13, 14, 15, 16, 17, 18, 19]). For instance, [20] introduction of mathematical modeling and best management of the anthracnose disease is a good example. Plant pathogen epidemiological models were examined by [21, 22, 23]. Foltso et al.[24] presented and analyzed a mathematical model of the coffee berry borer with optimal control strategies. The results were demonstrated using a class of models that had been subjected to plant disease experimentation. Following that, an impulse control approach that corresponds to cultivation methods was included to this study, making it more broadly applicable [25]. An important factor in the control of pests is farmer awareness, as demonstrated by [24, 26].

Coffee wilt disease, coffee leaf rust, and CBD are the three most dangerous coffee diseases that Ethiopia faces as a threat to its coffee production. The development and analysis of a nonlinear deterministic mathematical model for CBD transmission dynamics in a coffee farm was done by [27]. It was looked into how fungus pathogens interacted with disease vectors and coffee plants. Additionally, authors [28] developed a mathematical model of CBD dynamics. They determined the fundamental reproduction number (R_0), computed the equilibrium points of the system model, and showed that the CBD ends when $R_0 < 1$. Moreover, they have shown that if $R_0 > 1$, CBD remains in the population of coffee plants. The numerical simulation's results agree with stability analysis's theoretical conclusions.

For investigating the impact of the memory effect on epidemiological models [29] and generating more accurate results, fractional calculus is essential. Because fractional calculus was used so frequently, it was impossible to accurately depict a variety of inherited materials and memory processes in the framework of mathematical modeling [30]. Due to their special characteristics, fractional differential equations (FDE) provide a number of advantages over integer-order differential equations (IDEs) when it comes to simulating difficult real-world problems. Unlike (IDEs), which are based locally, FDEs are composed of memory effects, which contribute to their increased efficiency. In sense, it is more flexible than classical calculus because of its hereditary characteristics and the way memory is described [31, 32]. The Caputo fractional derivative (CFD), Caputo-Fabrizio derivative, Atangana-Baleanu fractional derivative, and many others are introduced in this tool for use in modeling. The various kernels available for fractional derivatives, which can be selected to meet the needs of various applications, are the fundamental differences between them. The key distinction between the Caputo fractional derivative [33], Caputo-Fabrizio derivative [34], and Atangana-Baleanu fractional derivative [35] is that the Caputo derivative is defined by a power law, the Caputo-Fabrizio derivative by an exponential decay law, and the Atangana-Baleanu derivative by a Mittag-Leffler law.

Fractional calculus has been investigated by numerous authors as having the potential to take the memory effect into account [36, 37, 38, 39, 40]. Based on data from the past and the present, this memory makes predictions. Compared to integer derivatives, this sets it apart. In order to handle issues in fractional calculus, which has numerous real-world applications[41], significant analytical and numerical approaches have been developed [42, 43, 44] and [45]. In fractional derivatives, several studies have recently been developed. One of the best operators is the Atangana Baleanu-Caputo (ABC) operator [46]. An expanded Mittag-Leffler function with a nonsingular and nonlocal kernel serves as the foundation for this operator.

Nevertheless, no previous research has used a fractional order to predict the kinetics of CBD transmission. In this work, we solve the CBD transmission dynamics' ABC fractional order model repeatedly. Furthermore, equilibria based on the value of the fundamental reproduction number (R_0) are studied with respect to their local and global asymptotic stability. The remaining sections of the paper are organized as follows: Some initial ideas and the model's formulation are covered in parts two and three, respectively. In parts four and five, respectively, the equilibrium points and stability analysis of CBD are established. Additionally, in parts six and seven, respectively, the numerical solution and numerical simulation of the model are examined. Part eight concludes with some final thoughts.

2 Preliminaries

Now let's begin by reviewing the fundamental definitions of Atangana-Baleanu fractional operators.
Definition 1: Let $f \in C^1(\alpha,\beta), \alpha < \beta$, be a function, and let $\sigma \in [0,1]$. The Atangana Baleanu (AB) fractional derivative in Caputo type of order σ is given by [47, 48]

$$ {}^{ABC}_{\alpha}D^{\sigma}_{t} f(t) = \frac{G(\sigma)}{1-\sigma}\int_{\alpha}^{t} \frac{df}{dn} E_{\sigma}\left[-\frac{\sigma}{1-\sigma}(t-n)^{\sigma}\right] dn, \tag{1} $$

where $G(\sigma)$ is the normalization function given by $G(\sigma) = 1-\sigma+\frac{\sigma}{\Gamma(\sigma)}$, characterized by $G(0) = G(1) = 1$, and the Mittag-Leffler function $E_{\sigma}(z)$ with $\mathbb{C}$ the set of the complex number is given by

$$ E_{\sigma}(z) = \sum_{b=0}^{\infty} \frac{z^b}{\Gamma(1+\sigma b)}, \sigma, b \in \mathbb{C}, \mathbb{R}(\sigma) > 0. \tag{2} $$

© 2025 NSP
Natural Sciences Publishing Cor.

Definition 2: The AB fractional integral of the function $f \in C^1(\alpha,\beta)$ is given by [47, 48]

$$ {}^{AB}_{\alpha}I^{\sigma}_{t} f(t) = \frac{1-\sigma}{G(\sigma)} f(t) + \frac{\sigma}{G(\sigma)\Gamma(\sigma)} \int_{\alpha}^{t} f(n)(t-n)^{\sigma-1} dn. \tag{3} $$

Lemma 1 [49]: The AB fractional derivative and AB fractional integral of the function $f \in C^1(\alpha,\beta)$ satisfies the Newton-Leibniz equality

$$ {}^{AB}_{\alpha}I^{\sigma}_{t} \left({}^{ABC}_{\alpha}D^{\sigma}_{t} f(t) \right) = f(t) - f(\alpha) $$

Lemma 2 [50]: For two functions $f, g \in \mathbb{K}^1(\alpha,\beta), \alpha < \beta$, the AB fractional derivative satisfies the following inequality:

$$ \| {}^{ABC}_{\alpha}D^{\sigma}_{t} f(t) - {}^{ABC}_{\alpha}D^{\sigma}_{t} g(t) \| \leq \mathbb{K} \| f(t) - g(t) \|. $$

3 Materials and Methods

3.1 Formulation of the Model

In this work, we partitioned the CBD model into coffee berry and vector populations. There are susceptible and infected coffee berry subcategories in the total coffee berry population $(N_c(t))$. Susceptible coffee berry is denoted by S_c, and infected coffee berry is denoted by I_c. This is defined as $N_c(t) = S_c + I_c$. There are susceptible and infected subclasses in the total vector population $(N_v(t))$. The susceptible vector is represented by S_v, and the infected vector is represented by I_v. This is defined as $N_v(t) = S_v + I_v$. The model took into account the recruitment rate of susceptible vectors r_2 and the shift to infected vectors (I_v) with β_2 rate after eating ill plants or coffee berry. The susceptible coffee berry (S_c) also replanted at rate r_1 and the diseases spread to coffee berry, when infected vectors (Y_v) eat susceptible coffee berry (S_c), the diseases propagate to coffee berry at a rate of β_1. coffee berry, once infected, never recovers and produces no or extremely low yields. To regulate the illness, the parameter γ is the induced death rate and is the elimination rate of infected coffee berry from uninfected coffee berry. Further more, d and μ are natural death rate of coffee berry and vector population respectively.
The following governing equations are given based on the model's assumptions:

$$ \begin{aligned} \frac{dS_c}{dt} &= r_1 - \beta_1 S_c I_v - d S_c, \\ \frac{dI_c}{dt} &= \beta_1 S_c I_v - (d+\gamma) I_c, \\ \frac{dS_v}{dt} &= r_2 - \beta_2 I_c S_v - \mu S_v, \\ \frac{dI_v}{dt} &= \beta_2 I_c S_v - \mu I_v. \end{aligned} \tag{4} $$

Now, replacing the $\frac{d}{dt}$ in the system (4) with ${}^{ABC}_{0}D^{\sigma}_{t}$, we obtain the AB derivative which is described by the system of differential equations given in equation (5).

$$ \begin{aligned} {}^{ABC}_{0}D^{\sigma}_{t} S_c(t) &= F_1(t, S_c), \\ {}^{ABC}_{0}D^{\sigma}_{t} I_c(t) &= F_2(t, I_c), \\ {}^{ABC}_{0}D^{\sigma}_{t} S_v(t) &= F_3(t, S_v), \\ {}^{ABC}_{0}D^{\sigma}_{t} I_v(t) &= F_4(t, I_v), \end{aligned} \tag{5} $$

where the kernels are given by

$$ \begin{aligned} F_1(t, S_c) &= r_1 - \beta_1 S_c I_v - d S_c, \\ F_2(t, I_c) &= \beta_1 S_c I_v - (d+\gamma) I_c, \\ F_3(t, S_v) &= r_2 - \beta_2 I_c S_v - \mu S_v, \\ F_4(t, I_v) &= \beta_2 I_c S_v - \mu I_v, \end{aligned} $$

with initial conditions

$$ S_c(0) > 0, I_c(0) \geq 0, S_v(0) \geq 0, I_v(0) \geq 0. \tag{6} $$

© 2025 NSP
Natural Sciences Publishing Cor.

3.2 Existence and Uniqueness of Solutions

The existence and uniqueness, nonnegativity, and boundedness of the solutions of the fractional-order model (5) are discussed in this section. To demonstrate the existence of the solution to model (5), we employ the well-known Banach fixed point theorem. We refer the reader to [51] and the references within it for a thorough examination of fixed points and contractions. To demonstrate the solution's existence and uniqueness, we proceed as follows. When we apply the ABC fractional integral to model (5), we get

$$\begin{aligned}
S_c(t)-S_c(0) &= \frac{1-\sigma}{\Gamma(\sigma)}F_1(t,S_c)+\frac{\sigma}{G(\sigma)\Gamma(\sigma)}\int_0^t F_1(\rho,S_c)(t-\rho)^{\sigma-1}d\rho,\\
I_c(t)-I_c(0) &= \frac{1-\sigma}{\Gamma(\sigma)}F_2(t,I_c)+\frac{\sigma}{G(\sigma)\Gamma(\sigma)}\int_0^t F_2(\rho,I_c)(t-\rho)^{\sigma-1}d\rho,\\
S_v(t)-S_v(0) &= \frac{1-\sigma}{\Gamma(\sigma)}F_3(t,S_v)+\frac{\sigma}{G(\sigma)\Gamma(\sigma)}\int_0^t F_3(\rho,S_v)(t-\rho)^{\sigma-1}d\rho,\\
I_v(t)-I_v(0) &= \frac{1-\sigma}{\Gamma(\sigma)}F_4(t,I_v)+\frac{\sigma}{G(\sigma)\Gamma(\sigma)}\int_0^t F_4(\rho,I_v)(t-\rho)^{\sigma-1}d\rho.
\end{aligned} \tag{7}$$

Consider the set $S = B(I)\times B(I)\times B(I)\times B(I)$ where $B(I) = C[0,T]$ is the Banach space of real-valued continuous functions defined on an interval $I = [0,T]$ with the corresponding norm defined by $\|S_c,I_c,S_v,I_v\| = \|S_c\|+\|I_c\|+\|S_v\|+\|I_v\|$, where

$$\|S_c\| = \sup_{t\in I}|S_c(t)|, \|I_c\| = \sup_{t\in I}|I_c(t)|, \|S_v\| = \sup_{t\in I}|S_v(t)|, \|I_v\| = \sup_{t\in I}|I_v(t)|.$$

Theorem 1 (Lipschitz condition and contraction): For each of the kernels F_1,F_2,F_3,F_4 in (5), there exists $V_i > 0, i = 1,2,3,4$, such that

$$\begin{aligned}
\|F_1(t,S_c)-F_1(t,S_{c\,1})\| &\le V_1\|S_c-S_{c\,1}(t)\|,\\
\|F_2(t,I_c)-F_2(t,I_{c\,1})\| &\le V_2\|I_c-I_{c\,1}(t)\|,\\
\|F_3(t,S_v)-F_3(t,S_{v\,1})\| &\le V_3\|S_v-S_{v\,1}(t)\|,\\
\|F_4(t,I_v)-F_4(t,I_{v\,1})\| &\le V_4\|I_v-I_{v\,1}(t)\|,
\end{aligned}$$

and are contractions for $0 \le V_i < 1, i = 1,2,3,4$.

Proof:

$$\begin{aligned}
\|F_1(t,S_c)-F_1(t,S_{c\,1})\| &= \|r_1-\beta_1 S_c I_v - dS_c-(r_1-\beta_1 S_{c\,1}I_v-dS_{c\,1})\|\\
&= \|-\alpha_1 S_c I_v - dS_c+\beta_1 S_{c\,1}I_v+dS_{c\,1}\|\\
&= \|\beta_1 I_v(S_{c\,1}-S_c)+d(S_{c\,1}-S_c)\|\\
&\le (\beta_1 n_1+d)\|(S_{c\,1}-S_c)\|\\
&\le V_1\|(S_{c\,1}-S_c)\|,
\end{aligned}$$

where $V_1 = \alpha_1 n_1 + d$.

$$\|S_c\| = \sup_{\tau\in I}|S_c(t)| = n_4, \|I_c\| = \sup_{\tau\in I}|I_c(t)| = n_3, \|S_v\| = \sup_{\tau\in I}|S_v(t)| = n_2, \|I_v\| = \sup_{\tau\in I}|I_v(t)| = n_1.$$

It then follows that $F_1(t,S_c)$ satisfies the Lipschitz condition with Lipschitz constant $V_1 = \alpha_1 n_1 + d$. Moreover, if $0 \le V_1 < 1$, then $F_1(t,S_c)$ is a contraction. In the same manner, we can show the existence of $V_i, i = 2,3,4$, and a contraction principle for $F_2(t,I_c),F_3(t,S_v),F_4(t,I_v), 0 \le V_i < 1$. Now for $t = t_n, n = 1,2,\ldots$, define the following recursive form of (7):

$$\begin{aligned}
S_c(t) &= \frac{1-\sigma}{G(\sigma)}F_1(t,S_{c\,n-1})+\frac{\sigma}{G(\sigma)\Gamma(\sigma)}\int_0^t F_1(t,S_{c\,n-1})(t-\rho)^{\sigma-1}d\rho,\\
I_c(t) &= \frac{1-\sigma}{G(\sigma)}F_2(t,S_{c\,n-1})+\frac{\sigma}{G(\sigma)\Gamma(\sigma)}\int_0^t F_2(t,I_{c\,n-1})(t-\rho)^{\sigma-1}d\rho,\\
S_v(t) &= \frac{1-\sigma}{G(\sigma)}F_3(t,S_{v\,n-1})+\frac{\sigma}{G(\sigma)\Gamma(\sigma)}\int_0^t F_3(t,S_{v\,n-1})(t-\rho)^{\sigma-1}d\rho,\\
I_v(t) &= \frac{1-\sigma}{G(\sigma)}F_4(t,I_{v\,n-1})+\frac{\sigma}{G(\sigma)\Gamma(\sigma)}\int_0^t F_4(t,I_{v\,n-1})(t-\rho)^{\sigma-1}d\rho,
\end{aligned} \tag{8}$$

© 2025 NSP
Natural Sciences Publishing Cor.

with initial conditions (6). In (8), the differences between successive terms are represented as follows:

$$\begin{aligned}
H_{1n}(t) =& S_{cn}(t) - S_{cn-1}(t),\\
=& \frac{1-\sigma}{G(\sigma)}\left(F_1(t,S_{cn-1}) - F_1(t,S_{cn-2})\right) + \frac{\sigma}{G(\sigma)\Gamma(\sigma)}\int_0^t \left(F_1(t,S_{cn-1}) - F_1(t,S_{cn-2})\right)(t-\rho)^{\sigma-1}d\rho,\\
H_{2n}(t) =& I_{cn}(t) - I_{cn-1}(t),\\
=& \frac{1-\sigma}{G(\sigma)}\left(F_2(t,I_{cn-1}) - F_2(t,I_{cn-2})\right) + \frac{\sigma}{G(\sigma)\Gamma(\sigma)}\int_0^t \left(F_2(t,I_{cn-1}) - F_2(t,I_{cn-2})\right)(t-\rho)^{\sigma-1}d\rho,\\
H_{3n}(t) =& S_{cn}(t) - S_{vn-1}(t),\\
=& \frac{1-\sigma}{G(\sigma)}\left(F_3(t,S_{vn-1}) - F_3(t,S_{vn-2})\right) + \frac{\sigma}{G(\sigma)\Gamma(\sigma)}\int_0^t \left(F_3(t,S_{vn-1}) - F_3(t,S_{vn-2})\right)(t-\rho)^{\sigma-1}d\rho,\\
H_{4n}(t) =& I_{vn}(t) - I_{vn-1}(t),\\
=& \frac{1-\sigma}{G(\sigma)}\left(F_4(t,I_{vn-1}) - F_4(t,I_{vn-2})\right) + \frac{\sigma}{G(\sigma)\Gamma(\sigma)}\int_0^t \left(F_4(t,I_{vn-1}) - F_4(t,I_{vn-2})\right)(t-\rho)^{\sigma-1}d\rho.
\end{aligned} \tag{9}$$

Taking the norm on both sides of each equation in (9), we have

$$\begin{aligned}
\|H_{1n}(t)\| =& \|S_{cn}(t) - S_{cn-1}(t)\|,\\
=& \frac{1-\sigma}{G(\sigma)}\|F_1(t,S_{cn-1}) - F_1(t,S_{cn-2})\| + \frac{\sigma}{G(\sigma)\Gamma(\sigma)}\int_0^t \|F_1(t,S_{cn-1}) - F_1(t,S_{cn-2})\|(t-\rho)^{\sigma-1}d\rho,\\
\|H_{2n}(t)\| =& \|I_{cn}(t) - I_{cn-1}(t)\|,\\
=& \frac{1-\sigma}{G(\sigma)}\|F_2(t,I_{cn-1}) - F_2(t,I_{cn-2})\| + \frac{\sigma}{G(\sigma)\Gamma(\sigma)}\int_0^t \|F_2(t,I_{cn-1}) - F_2(t,I_{cn-2})\|(t-\rho)^{\sigma-1}d\rho,\\
\|H_{3n}(t)\| =& \|S_{cn}(t) - S_{vn-1}(t)\| = \frac{1-\sigma}{G(\sigma)}\|F_3(t,S_{vn-1}) - F_3(t,S_{vn-2})\|\\
&+ \frac{\sigma}{G(\sigma)\Gamma(\sigma)}\int_0^t \|F_3(t,S_{vn-1}) - F_3(t,S_{vn-2})\|(t-\rho)^{\sigma-1}d\rho,\\
\|H_{4n}(t)\| =& \|I_{vn}(t) - I_{vn-1}(t)\|,\\
=& \frac{1-\sigma}{G(\sigma)}\|F_4(t,I_{vn-1}) - F_4(t,I_{vn-2})\| + \frac{\sigma}{G(\sigma)\Gamma(\sigma)}\int_0^t \|F_4(t,I_{vn-1}) - F_4(t,I_{vn-2})\|(t-\rho)^{\sigma-1}d\rho.
\end{aligned} \tag{10}$$

Furthermore, the first equality in (10) can be reduced to the following expressions:

$$\begin{aligned}
\|H_{1n}(t)\| =& \|S_{cn}(t) - S_{cn-1}(t)\|,\\
\leq& \frac{1-\sigma}{G(\sigma)}\|F_1(t,S_{cn-1}) - F_1(t,S_{cn-2})\| + \frac{\sigma}{G(\sigma)\Gamma(\sigma)}\int_0^\tau \|F_1(t,S_{cn-1}) - F_1(t,S_{cn-2})\|(t-\rho)^{\sigma-1}d\rho,\\
\leq& \frac{1-\sigma}{G(\sigma)}V_1\|S_{cn-1}) - S_{cn-2})\| + \frac{\sigma}{G(\sigma)\Gamma(\sigma)}\int_0^\tau \|S_{cn-1}) - S_{cn-2})\|(t-\rho)^{\sigma-1}d\rho,\\
\leq& V_1\|H_{1(n-1)}(t)\|\left|\frac{1-\sigma}{G(\sigma)} + \frac{t^\sigma}{G(\sigma)\Gamma(\sigma)}\right|.
\end{aligned} \tag{11}$$

As a result, we have

$$\|H_{1n}(t)\| \leq V_1\left|\frac{1-\sigma}{G(\sigma)} + \frac{t^\sigma}{G(\sigma)\Gamma(\sigma)}\right|\|H_{1(n-1)}(t)\|. \tag{12}$$

Similarly, the leftover expressions of (10) can be simplified to the following:

$$\begin{aligned}
\|H_{2n}(t)\| &\leq V_2\left|\frac{1-\sigma}{G(\sigma)} + \frac{t^\sigma}{G(\sigma)\Gamma(\sigma)}\right|\|H_{2(n-1)}(t)\|,\\
\|H_{3n}(t)\| &\leq V_3\left|\frac{1-\sigma}{G(\sigma)} + \frac{t^\sigma}{G(\sigma)\Gamma(\sigma)}\right|\|H_{3(n-1)}(t)\|,\\
\|H_{4n}(t)\| &\leq V_4\left|\frac{1-\sigma}{G(\sigma)} + \frac{t^\sigma}{G(\sigma)\Gamma(\sigma)}\right|\|H_{4(n-1)}(t)\|.
\end{aligned} \tag{13}$$

© 2025 NSP
Natural Sciences Publishing Cor.

Theorem 2: If we can find Π_0^σ that satisfies the inequality, the ABC fractional model given in (5) has a solution.

$$\left(\frac{1-\sigma}{G(\sigma)}+\frac{\Pi_0^\sigma}{G(\sigma)\Gamma(\sigma)}\right)V_i<1, i=1,2,3,4. \tag{14}$$

Proof: From (12) and (13) we have

$$\begin{aligned}
\|H_{1n}(t)\| &\leq \|S_c(0)\|\left[\left(\frac{1-\sigma}{G(\sigma)}+\frac{\Pi_0^\sigma}{G(\sigma)\Gamma(\sigma)}\right)V_1\right]^n,\\
\|H_{2n}(t)\| &\leq \|I_c(0)\|\left[\left(\frac{1-\sigma}{G(\sigma)}+\frac{\Pi_0^\sigma}{G(\sigma)\Gamma(\sigma)}\right)V_2\right]^n,\\
\|H_{3n}(t)\| &\leq \|S_v(0)\|\left[\left(\frac{1-\sigma}{G(\sigma)}+\frac{\Pi_0^\sigma}{G(\sigma)\Gamma(\sigma)}\right)V_3\right]^n,\\
\|H_{4n}(t)\| &\leq \|I_v(0)\|\left[\left(\frac{1-\sigma}{G(\sigma)}+\frac{\Pi_0^\sigma}{G(\sigma)\Gamma(\sigma)}\right)V_4\right]^n.
\end{aligned} \tag{15}$$

Theorem 1 confirms the existence of the solution (the existence of a fixed point), and we have to show that the functions $S_c(t), I_c(t), S_v(t), I_v(t)$ are solutions of model (5). Assume the following conditions are met:

$$\begin{aligned}
S_c(t)-S_c(0) &= S_{c\,n}(t)-h_{1n}(t),\\
I_c(t)-I_c(0) &= I_{c\,n}(t)-h_{2n}(t),\\
S_v(t)-S_v(0) &= S_{v\,n}(t)-h_{3n}(t),\\
I_v(t)-I_v(0) &= I_{v\,n}(t)-h_{4n}(t).
\end{aligned} \tag{16}$$

From (16) we obtain

$$\begin{aligned}
\|h_{1n}(t)\| &\leq \frac{1-\sigma}{G(\sigma)}\|\left(F_1(\tau,S_{c\,n})-F_1(\tau,S_{c\,n-1})\right)\|(\tau-\rho)^{\sigma-1}d\rho,\\
&\leq \frac{1-\sigma}{G(\sigma)}V_1\|S_{c\,n}-S_{c\,n-1}\|+\frac{\sigma^n}{G(\sigma)\Gamma(\sigma)}V_1\|S_{c\,n}-S_{c\,n-1}\|.
\end{aligned} \tag{17}$$

Recursion of the process results in

$$\|h_{1n}(t)\| \leq \left[\frac{1-\sigma}{G(\sigma)}+\frac{t^\sigma}{G(\sigma)\Gamma(\sigma)}\right]^{n+1}V_1^n\|S_{c\,n}-S_{c\,n-1}\|^n$$

which at $t=\Pi_0^\sigma$ yields

$$\begin{aligned}
&\|h_{1n}(t)\| \leq \left[\frac{1-\sigma}{G(\sigma)}+\frac{\Pi_0^\sigma}{G(\sigma)\Gamma(\sigma)}\right]^{n+1}V_1^n\|S_{c\,n}-S_{c\,n-1}\|^n,\\
&\|h_{1n}(t)\| \to 0.
\end{aligned} \tag{18}$$

Applying the limit to both sides of (18) as $n\to\infty$, we see that $\|h_{1n}(t)\|\to 0$ for

$$\left[\frac{1-\sigma}{G(\sigma)}+\frac{t^\sigma}{G(\sigma)\Gamma(\sigma)}\right]V_1<1.$$

Similarly, we can show that $\|h_{2n}(t)\|\to 0, \|h_{3n}(t)\|\to 0, \|h_{4n}(t)\|\to 0,$

$$\left[\frac{1-\sigma}{G(\sigma)}+\frac{t^\sigma}{G(\sigma)\Gamma(\sigma)}\right]V_i, 1i=2,3,4.$$

The Banach fixed point theorem guarantees the existence of the solution of model (5). The solution's uniqueness is demonstrated in Theorem 3.

Theorem 3 (Uniqueness of solution): The AB fractional model (5) has a unique solution if

$$\left[\frac{1-\sigma}{G(\sigma)}+\frac{t^\sigma}{G(\sigma)\Gamma(\sigma)}\right]V_i, \quad i=1,2,3,4. \tag{19}$$

© 2025 NSP
Natural Sciences Publishing Cor.

Proof: Let us assume that $S_{c\,1}(t), I_{c\,1}(t) S_{v\,1}(t), I_{v\,1}(t)$ are also solutions to (5). Then

$$S_c(t) - S_{c\,1}(t) = \frac{1-\sigma}{G(\sigma)} \left(F_1(t, S_c) - F_1(t, S_{c\,1})\right) + \frac{\sigma}{G(\sigma)\Gamma(\sigma)} \int_0^t \left(F_1(t, S_c) - F_1(t, S_{c\,1})\right) (t-\rho)^{\sigma-1} d\rho.$$

Taking the norm of both sides, we obtain

$$\|S_c(t) - S_{c\,1}(t)\| = \frac{1-\sigma}{G(\sigma)} V_1 \|S_c - S_{c\,1}\| + \frac{t^\sigma}{G(\sigma)\Gamma(\sigma)} V_1 \|S_c - S_{c\,1}\|.$$

Since $\left(1 - V_1 \left(\frac{1-\sigma}{G(\sigma)} + \frac{t^\sigma}{G(\sigma)\Gamma(\sigma)}\right)\right) > 0$, we obtain $\|S_c(t) - S_{c\,1}(t)\| = 0$. Thus we have $S_c(t) = S_{c\,1}(t)$. Similarly, we can show that $I_c(t) = I_{c\,1}(t), S_v(t) = S_{v\,1}(t), I_v = I_{v\,1}(t)$, which completes the proof of Theorem 3.

Lemma 3 (Generalized mean value theorem, [52]): Let $f(x) \in C[\alpha, \beta]$, and let ${}_0^{ABC}D_t^\sigma f(x) \in C[\alpha, \beta]$ when $0 < \sigma \leq 1$. Then we have $f(x) = f(\alpha) + \frac{1}{\Gamma(\sigma)} {}_0^{ABC}D_t^\sigma f(\phi)(x-\phi)^n$, when $0 \leq \phi \leq x, \forall x \in (\alpha, \beta]$. Note that by Lemma 3, if $f(x) \in [0, \beta]$, ${}_0^{ABC}D_t^\sigma f(x) \in C[0, \beta]$ and ${}_0^{ABC}D_t^\sigma f(x) \geq 0, \forall x \in (0, \beta]$ when $0 \leq \sigma \leq 1$, then the function $f(x)$ is nondecreasing, and if ${}_0^{ABC}D_t^\sigma f(x) \leq 0, \forall x \in (0, \beta]$ then the function g(x) is nonincreasing $\forall x \in (0, \beta]$.

Theorem 4: The epidemiologically feasible region of *AB* model (5) is given by:

$$\Omega = \Omega_c \times \Omega_v = \left\{ (S_c, I_c, S_v, I_v) \in \mathbb{R}_+^4 : N_c \leq \frac{r_1}{d}, N_v \leq \frac{r_1}{\mu} \right\}. \tag{20}$$

Proof: Using Lemma 3, we have

$$\begin{aligned}
{}_0^{ABC}D_t^\sigma S_c|_{S_c=0} &= r_1 \geq 0, \\
{}_0^{ABC}D_t^\sigma I_c|_{I_c=0} &= \beta_1 S_c I_v \geq 0, \\
{}_0^{ABC}D_t^\sigma S_v|_{S_v=0} &= r_2 \geq 0, \\
{}_0^{ABC}D_t^\sigma S_v|_{I_v=0} &= \beta_2 I_c S_v \geq 0.
\end{aligned} \tag{21}$$

It follows from (21) that each of the solutions of (5) is nonnegative and remains in $\mathbb{R}_+^4$, and hence the set Ω defined in (20) is positively invariant for model (5). Eventually, to demonstrate the boundedness of the fractional model's solutions (5), given that all of the parameters are positive, we continue by adding up all of the model's equations for both cotton and vector population, which yields:

$${}_0^{ABC}D_t^\sigma N_c = r_1 - dN_c - \gamma I_c \leq r_1 - dN_c, \tag{22}$$

$${}_0^{ABC}D_t^\sigma N_v = r_2 - \mu N_v. \tag{23}$$

Now, using the Laplace transform and simplifying equations (22) and (23), we get

$$\begin{aligned}
N_c(t) \leq & \left(\frac{G(\sigma)}{G(\sigma) + (1-\sigma)d} N_c(0) + \frac{(1-\sigma) r_1}{G(\sigma) + (1-\sigma)d} \right) E_{\sigma,1}\left(-c_1 t^\sigma\right) \\
& + \frac{\sigma r_1}{G(\sigma) + (1-\sigma)d} E_{\sigma,\sigma+1}\left(-c_2 t^\sigma\right),
\end{aligned} \tag{24}$$

$$\begin{aligned}
N_v(t) \leq & \left(\frac{G(\sigma)}{G(\sigma) + (1-\sigma)\mu} N_v(0) + \frac{(1-\sigma) r_2}{G(\sigma) + (1-\sigma)\mu} \right) E_{\sigma,1}\left(-c_2 t^\sigma\right) \\
& + \frac{\sigma r_2}{G(\sigma) + (1-\sigma)\psi} E_{\sigma,\sigma+1}\left(-c_2 t^\sigma\right),
\end{aligned} \tag{25}$$

where $c_1 = \frac{\sigma d}{G(\sigma)+(1-\sigma)d}$ and $c_2 = \frac{\sigma \mu}{G(\sigma)+(1-\sigma)\mu}$ with E_{σ,c_1} and E_{σ,c_2} constitute the two parameter Mittag-Leffler function and due to its asymptotic nature which leads to the conclusion that $N_c(t) \leq \frac{r_1}{d}$ and $N_v(t) \leq \frac{r_2}{\mu} ast \to \infty$. Hence (20) is the biologically feasible region of model (5).

© 2025 NSP
Natural Sciences Publishing Cor.

3.3 Equilibrium Points of the Model

3.3.1 The Coffee Berry Disease-Free Equilibrium Points of the Model (E_0)

The coffee berry disease-free equilibrium points (E_0) of the model are stationary solutions with no diseases. It is obtained by equating equation (5) to zero and using $I_c = 0$ and $Y_v = 0$. Then, E_0 of our model equation (5) is given by:

$$E_0 = (S_c^0, I_c^0, S_v^0, I_v^0) = \left(\frac{r_1}{d}, 0, \frac{r_2}{\mu}, 0\right). \tag{26}$$

3.3.2 The Basic Reproduction Number (R_0)

The basic reproduction number (R_0) counts the estimated number of secondary infections that result from one newly infected coffee berry delivered directly into a susceptible population. Then, by the principle of next generation matrix, basic reproduction number (R_0) is the dominant eigen value of the FV^{-1} or spectral radius of FV^{-1} where

$$\mathrm{F} = \begin{pmatrix} 0 & \frac{\beta_1 r_1}{d} \\ \frac{\beta_2 r_2}{\mu} & 0 \end{pmatrix}, \mathrm{V} = \begin{pmatrix} \frac{1}{d+\gamma} & 0 \\ 0 & \frac{1}{\mu} \end{pmatrix}. \tag{27}$$

After simplification, we obtain

$$R_0 = \sqrt{\frac{r_1 r_2 \beta_1 \beta_2}{(d+\gamma) d \mu^2}}. \tag{28}$$

3.3.3 Coffee Berry Disease Endemic Equilibrium Point of the Model (E_1)

The coffee berry endemic equilibrium point, $E_1 = (S_c^*, I_c^*, S_v^*, I_v^*)$ of the model is the steady state solution where coffee berry persist in the population of coffee plants. We can obtain by equating each system of the equation (5) equal to zero and it is given by:

$$S_c^* = \frac{r_1(r_1\beta_2 + \mu(d+\gamma))}{d\mu(d+\gamma)(R_0^2-1) + d(r_1\beta_2 + \mu(d+\gamma))}, \tag{29}$$

$$I_c^* = \frac{r_1\mu(R_0^2-1)}{\mu((d+\gamma))(R_0^2-1) + (r_1\beta_2 + \mu(d+\gamma))}, \tag{30}$$

$$S_v^* = \frac{r_2((d+\gamma)\mu(R_0^2-1) + r_1\beta_2 + d\mu)}{\mu((r_1\beta_2 + d\mu)(R_0^2-1) + r_1\beta_2 + \mu(d+\gamma))}, \tag{31}$$

$$I_v^* = \frac{d\mu(d+\gamma)(R_0^2-1)}{\beta_1(r_1\beta_2 + \mu)(d+\gamma)}. \tag{32}$$

3.4 Stability Analysis of the Model

3.4.1 Local Stability of the Coffee Berry Disease Free Equilibrium Point

The linearization system of equation (5) at E_0 can be used to find the local stability of the model at E_0.
Theorem 5: Disease free equilibrium point (E_0) of system of equation (5) is locally asymptotically stable, if $R_0 < 1$.
Proof. Evaluating the Jacobian matrix of system of equation (5) at $E_0 = \left(\frac{r_1}{d}, 0, \frac{r_2}{\mu}, 0\right)$ is

$$J(E_0) = \begin{pmatrix} -d & 0 & 0 & -\frac{\beta_1 r_1}{d} \\ 0 & -(d+\gamma) & 0 & \frac{\beta_1 r_1}{d} \\ 0 & -\frac{\beta_2 r_2}{\mu} & -\mu & 0 \\ 0 & \frac{\beta_2 r_2}{\mu} & 0 & -\mu \end{pmatrix}. \tag{33}$$

© 2025 NSP
Natural Sciences Publishing Cor.

The corresponding characteristic equation of Jacobian matrix of equation (33) at E_0 is given by $|J(E_0)-\lambda I_4|=0$. That is

$$(-d-\lambda)(-\mu-\lambda)(\lambda^2+d_1\lambda+d_2)=0. \tag{34}$$

where

$$\begin{aligned} d_1 &= d+\gamma+\mu, \\ d_2 &= (d+\gamma)\mu-\frac{r_1r_2\beta_1\beta_2}{d\mu}=(d+\gamma)\mu\left[1-\frac{r_1r_2\beta_1\beta_2}{(d+\gamma)d\mu^2}\right]=(d+\gamma)\mu(1-R_0^2). \end{aligned} \tag{35}$$

Clearly, from equation (34), we observe that

$$\lambda_1=-d<0, \lambda_2=-\mu<0, \tag{36}$$

and from the last expression of equation (34) , that is

$$\lambda^2+d_1\lambda+d_2=0, \tag{37}$$

by using the Routh-Hurwitz criteria, equation (37) has strictly negative real root if $d_1>0$ and $d_2>0$. Clearly, we observe that $d_1=d+\gamma+\mu>0$ and

$$d_2=(d+\gamma)\mu(1-R_0^2)>0, \tag{38}$$

if $(1-R_0^2)>0$. That is $R_0^2<1$ implies that $R_0<1$. As a result, our model equation (5) at E_0 offers all eigenvalues with a negative real part, and so it is locally asymptotically stable if $R_0<1$.

3.4.2 Global Stability of the Coffee Berry Disease Free Equilibrium Point

To establish the global stability of disease free equilibrium point (E_0), we need to rewrite the system of equation (5) in the following form:

$$\begin{aligned} \dot{M} &= J(M,L), \\ \dot{L} &= P(M,L), \\ P(M,0) &= 0, \end{aligned} \tag{39}$$

where $M=(S_c,S_v)\in R^2$ represent the number of uninfected classes, while, $L=(I_c,I_v)\in R^2$ represent the number of infected classes and $E_0=(M^0,0)$ represents the coffee berry disease-free equilibrium of this system. The disease-free equilibrium E_0 is globally asymptotically stable equilibrium for the model if the following conditions are fulfilled:

1. $\frac{dM}{dt}=J(M,0), M^*$ is globally asymptotically stable.
2. $\frac{dL}{dt}=D_LP(M^*,0)L-P_1(M,L), P_1(M,L)\geq 0, \forall (M,L)\in\Omega$.

where $D_LP(M^0,0)$ is an M-matrix and $P(M,L)$ taken in (I_c,Y_v) and evaluated at $(M^0,0)=\left(\frac{r_1}{d},\frac{r_2}{\mu},0,0\right)$. If system of equation (39) satisfies the above conditions, then the following theorem holds.

Theorem 6: The coffee berry disease free equilibrium point, $E_0=(M^0,0)$ of system of equation (5) is globally asymptotically stable if $R_0\leq 1$ and conditions (1) and (2) are holds.

Proof: From our model of equation (5), we can obtain $J(M,L)$ and $P(M,L)$:

$$J(M,L)=\begin{pmatrix} r_1-\beta_1S_cI_v-dS_c \\ r_2-\beta_2I_cS_v-\mu S_v \end{pmatrix},$$

$$P(M,L)=\begin{pmatrix} \beta_1S_cI_v-(d+\gamma)I_c \\ \beta_2I_cS_v-\mu I_v \end{pmatrix}.$$

Now, we consider the reduced system and from condition (1)

$$ {}_0^{ABC}D_t^{\sigma}S_c=r_1-dS_c, \tag{40}$$

$$ {}_0^{ABC}D_t^{\sigma}S_v=r_2-\mu S_v, \tag{41}$$

© 2025 NSP
Natural Sciences Publishing Cor.

$M^0 = \left(\frac{r_1}{d}, \frac{r_2}{\mu}\right)$ is a globally asymptotically stable equilibrium point for the reduced system $\frac{dM}{dt} = J(M,0)$. This can be verified from the solution of the equation (40); we get $S_c(t) = \frac{r_1}{d} + \left(S_c(0) - \frac{r_1}{d}\right)e^{-dt}$ which approaches $\frac{r_1}{d}$ as $t \to \infty$ and from equation (41), we obtain $S_v(t) = \frac{r_2}{\psi} + (S_v(0) - \frac{r_2}{\mu})e^{-\mu t}$ which approaches $\frac{r_2}{\mu}$ as $t \to \infty$. Note that this asymptomatic dynamics is independent of the initial conditions in Ω; therefore the convergence of the solutions of the reduced system (40) and (41) is global in Ω. Now, we compute

$$D_L P(M^0,0) = \begin{pmatrix} -(d+\gamma) & \frac{r_1\beta_1}{d} \\ \frac{r_2\beta_2}{\mu} & -\mu \end{pmatrix}. \tag{42}$$

Then, $P(M,L)$ can be written as

$$P(M,L) = D_L P(M^*,0)L - P_1(M,L), \tag{43}$$

and we want to show $P_1(M,L)$, which is obtained as

$$P_1(M,L) = \begin{pmatrix} \beta_1 I_v \left(\frac{r_1}{d} - S_c\right) \\ \beta_2 I_c \left(\frac{r_2}{\mu} - S_v\right) \end{pmatrix}. \tag{44}$$

Here $\frac{r_1}{d} \geq S_c$ and $\frac{r_2}{\mu} \geq S_v$. Hence it is clear that $P_1(M,L) \geq 0$, $\forall (M,L) \in \Omega$. Thus, this proves that E_0 is globally asymptotically stable when $R_0 \leq 1$.

3.4.3 Local Stability of the Coffee Berry Endemic Equilibrium Point

We used the Jacobian stability approach to prove the local stability of the disease endemic equilibrium state in this section.
Theorem 7: When $R_0 > 1$, the model's endemic equilibrium point, E_1, is locally asymptotically stable.
Proof: The local stability of the coffee berry endemic equilibrium (E_1), is determined based on the signs of the eigenvalues of the Jacobian matrix which is computed at E_1. Now, the Jacobian matrix of the our model at E_1 is given by:

$$J = \begin{pmatrix} -(\beta_1 I_v^* + d) & 0 & 0 & -\beta_1 S_c^* \\ \beta_1 I_v^* & -(d+\gamma) & 0 & \beta_1 S_c^* \\ 0 & -\beta_2 S_v^* & -(\beta_2 I_c^* + \mu) & 0 \\ 0 & \beta_2 S_v^* & \beta_2 I_c^* & -\mu \end{pmatrix}. \tag{45}$$

The corresponding characteristic equation of Jacobian matrix of equation (45) at E_1 is $|J(E_1) - \lambda I_4| = 0$. That is

$$P(\lambda) = f_4\lambda^4 + f_3\lambda^3 + f_2\lambda^2 + f_1\lambda + f_0, \tag{46}$$

where

$$\begin{aligned} f_4 =& 1, f_3 = 2d + 2\mu + \beta_1 I_v^* + \beta_2 I_c^*, \\ f_2 =& d\mu + (d+\mu)(d+\gamma+\mu)(d+\gamma)\mu + (2\mu+d)\beta_1 I_v^* + (2d+\mu)\beta_2 I_c^* + \beta_1\beta_2(I_c^* - S_c^* I_v^*), \\ f_1 =& \mu d(d+\gamma+\mu) + (d+\mu)(d+\gamma)\mu + (d\mu + (d+\mu)(d+\gamma))\beta_2 I_c^* + (d+\gamma+\mu)\mu\beta_1 I_v^* \\ & + (d+\mu)\beta_1\beta_2 I_c^* I_v^* - \beta_1\beta_2(d+\mu)S_c^* S_v^*, \\ f_0 =& \mu\beta_1\beta_2(d+\gamma)I_c^* S_v^* + \beta_1\mu^2(d+\gamma)I_v^* + \mu\beta_1\beta_2(d+\gamma)I_c^* + d\mu^2(d+\gamma) - d\mu\beta_1\beta_2 S_c^* S_v^*. \end{aligned} \tag{47}$$

Using the Routh-Hurwitz criterion, all roots of characteristic polynomial have negative real parts if and only if $f_4 > 0, f_3 > 0, f_2 > 0, f_1 > 0, f_0 >, f_3 f_2 > f_1$ and $f_1 f_2 f_3 > f_0 f_3^2 + f_1^2$ for $R_0 > 1$. Therefore, E_1 is locally asymptotically stable if $R_0 > 1$.

4 Numerical Results and Discussions

This section examines the effects of various fractional order values on the system of equations (5). The following initial conditions and parameters values are used in the simulations and analysis which are taken from literatures and assumptions: $S_c(0) = 700, I_c(0) = 150, S_v(0) = 100, I_v(0) = 180, r_1 = 9, r_2 = 5, \beta_1 = 0.0004, \beta_2 = 0.0005, d = 0.04$ and $\mu = 0.009$. Figure 1 depicts how populations of susceptible coffee berries rise asymptotically to the disease-free

© 2025 NSP
Natural Sciences Publishing Cor.

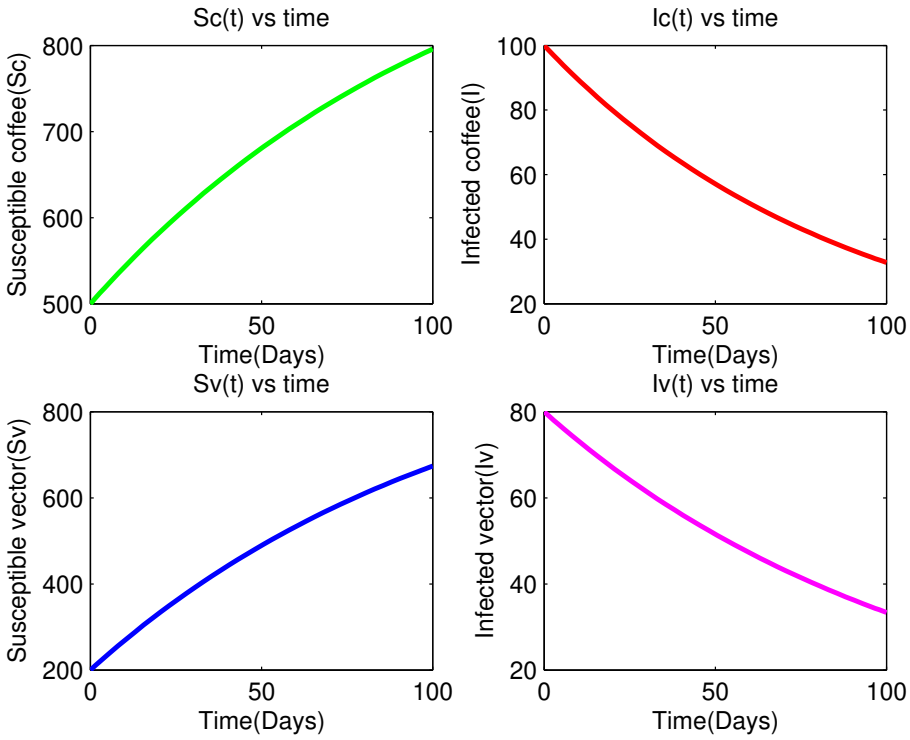

Fig. 1: Time series plot of state variables for $R_0 < 1$

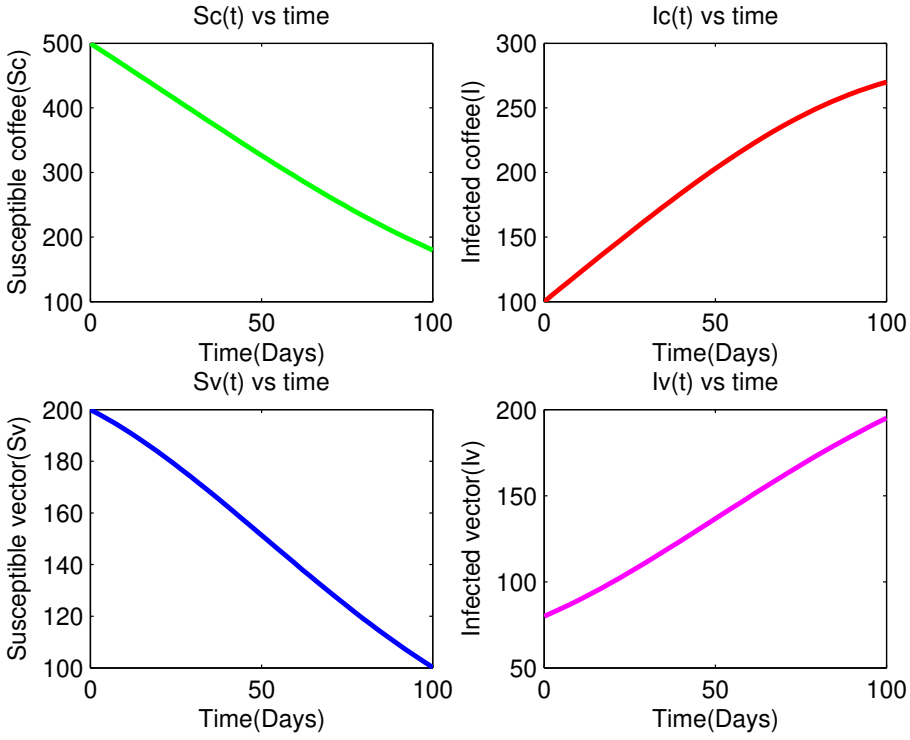

Fig. 2: Time series plot of state variables for $R_0 > 1$

© 2025 NSP
Natural Sciences Publishing Cor.

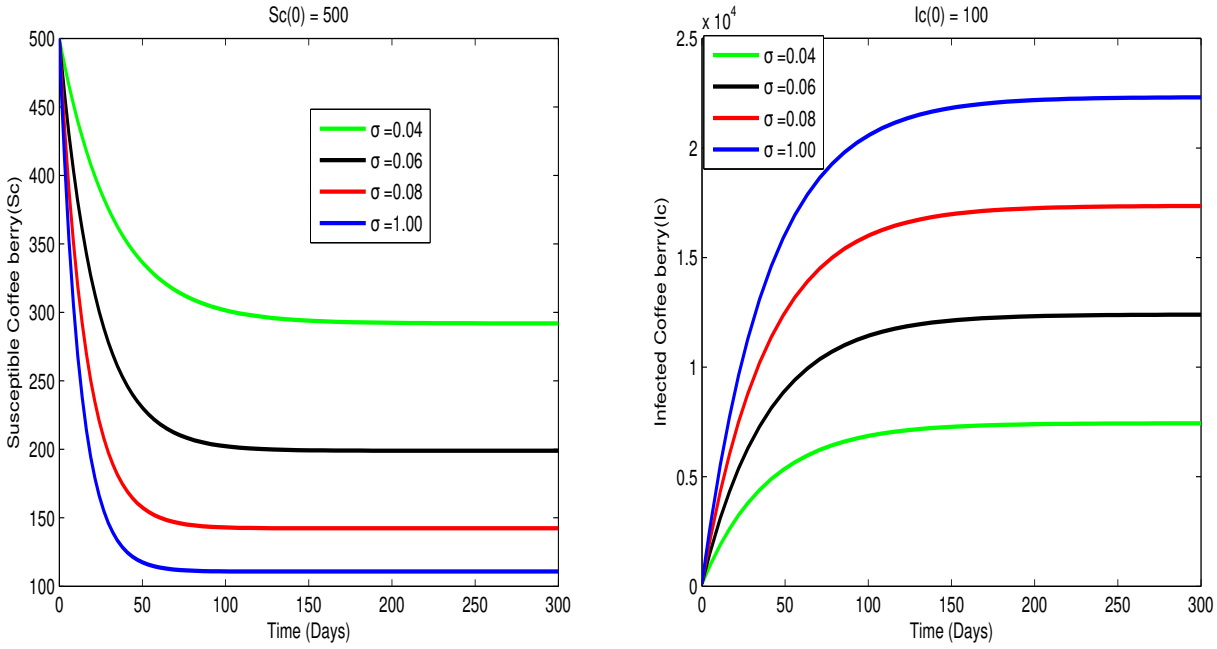

(a) **(b)**

Fig. 3: Total number of susceptible and infected coffee berry with different values of σ.

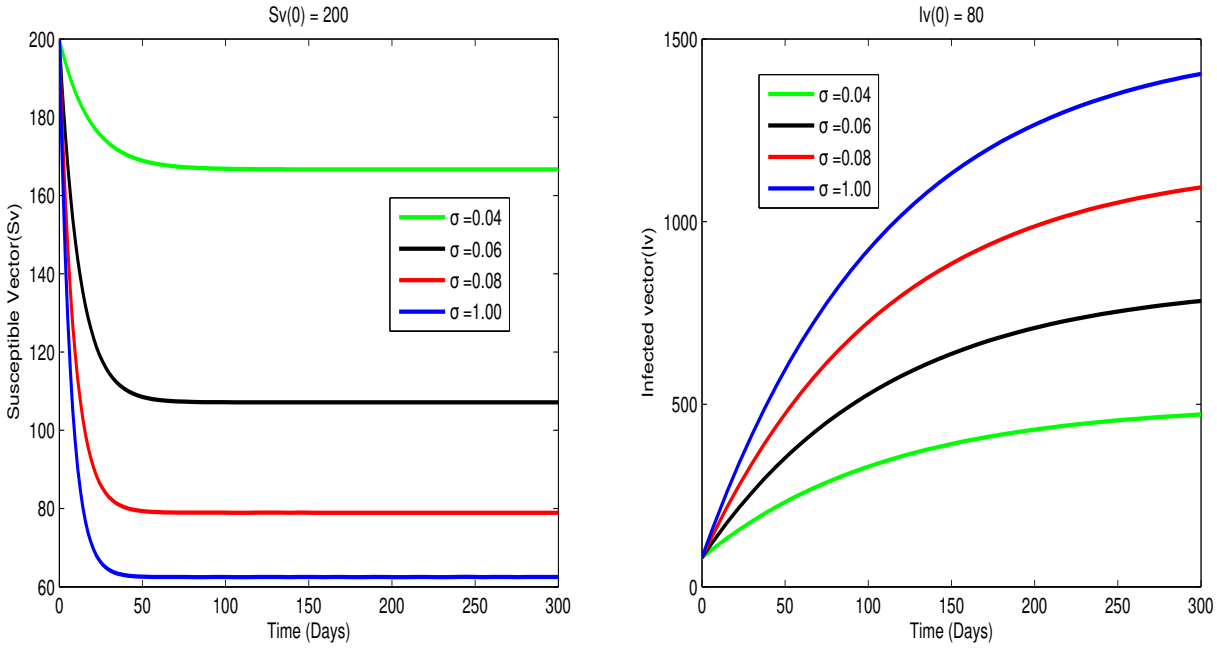

(a) **(b)**

Fig. 4: Total number of susceptible and infected vector with different values of σ.

© 2025 NSP
Natural Sciences Publishing Cor.

equilibrium point while those of infected coffee berries fall asymptotically to that point. The susceptible vector population increases asymptotically to the disease-free equilibrium point, whereas the infected vector population decreases asymptotically to the same equilibrium point. In this case, the disease might ultimately go away in the long run. The fact that $R_0 = 0.0442$, which is less than one, accounts for the existence of such a condition. This indicates the theorem that the stability of the disease-free equilibrium point occurs when $R_0 < 1$, i.e., if $R_0 < 1$, then on average, one infected coffee berry produces less than one newly infectious coffee berry over the course of its disease period. Figure 2 demonstrates how the number of susceptible coffee berry and vector decreases as a result of the influence of infected coffee berry and vector people, after which they join the infected class, leading to an increase in infected coffee berry and vector. As a result, the number of infected coffee berries and vectors is rising, and the disease's endemic equilibrium point is both present and stable. The fact that $R_0 = 5.3244$, which is greater than one, proves that this condition exists. This demonstrates the theorem that disease endemic equilibrium points are stable when $R_0 > 1$, i.e., if each infected coffee berry and its vectors produce, on average, more than one new infected coffee berry and vector, then disease can spread in the specified area. Figure 3a demonstrates how decreasing the number of coffee berries (S_c) that are susceptible results from increasing the fractional order (σ) from 0.04 to 1.00. Figure 3b demonstrates how increasing the fractional order (σ) from 0.04 to 1.00 results in an increase in the number of infected coffee berries (I_c). According to Figure 4a, the number of susceptible vector populations (S_v) decreases as fractional order (σ), increases from 0.04 to 1.00. The fractional order (σ) is shown in Figure 4b to increase from 0.04 to 1.00, which results in an increase in the population of infected vectors (I_v). To put it another way, we can infer from figures 3 - 4 that a reduction in σ results in a marked decrease in the number of I_c and I_v cases. The curves for each compartment, I_c and I_v, also compress as the value decreases from 1.00 to 0.04, as shown in the figures. Therefore, we can say that diseases in I_c and I_v decrease as one approaches zero from the right.

5 Conclusion

In this study, we looked into an Atangana Baleanu fractional derivative-based mathematical model for eco-epidemiology. We established the existence and uniqueness of the solution, asymptotic stability of the equilibria, and the fundamental reproduction number (R_0). The findings of the study, the coffee berry disease-free equilibrium is locally and globally asymptotically stable if the basic reproduction number is less than one; however, if the basic reproduction number is greater than one, the coffee berry endemic equilibrium is locally asymptotically stable. According to the simulation results, the graphs flattened as the fractional derivative order was decreased from 1.00, and the disease progresses slowly for the susceptible class (S_c). The graphs for compartments (I_c) and (I_v) demonstrate that the disease spread gradually as the fractional order deviates from 1.00, and the number of cases at maximum declines relatively. This noteworthy results is due to the fractional operator Atangana Baleanu with the inherited assets. We claim that fractional models using the Atangana Baleanu operator can shed more light on the hidden or actual characteristics of phenomena encountered in everyday life. As the order is decreased, we see a decrease in the number of cases as we display graphic results with various fractional orders. The impact of other fractional operators like Caputo-Fabrizio fractional derivatives, and comparisons with the Atangana-Baleanu fractional operator lead on the same model or other relevant models. In the future, we can update our model by taking optimal control into account, and we can investigate the resulting new model using various kinds of fractional order operators.

References

[1] O. Sujaritpong, S. Yoo-Kong, P. Bhadola, Analysis and dynamics of the international coffee trade network, in: Journal of Physics: Conference Series, Vol. 1719, IOP Publishing, 2021, p. 012106.
[2] W. Garedew, F. Lemessa, F. Pinard, Assessment of berry drop due to coffee berry disease and non-cbd factors in arabica coffee under farmers fields of southwestern ethiopia, Crop protection 98 (2017) 276–282.
[3] A. Vieira, D. N. Silva, V. Várzea, O. S. Paulo, D. Batista, Novel insights on colonization routes and evolutionary potential of colletotrichum kahawae, a severe pathogen of coffea arabica, Molecular plant pathology 19 (11) (2018) 2488–2501.
[4] D. Batista, D. N. Silva, A. Vieira, A. Cabral, A. S. Pires, A. Loureiro, L. Guerra-Guimaraes, A. P. Pereira, H. Azinheira, P. Talhinhas, et al., Legitimacy and implications of reducing colletotrichum kahawae to subspecies in plant pathology, Frontiers in plant science 7 (2017) 2051.
[5] J. Mouen Bedimo, D. Bieysse, S. Nyassé, J.-L. Notteghem, C. Cilas, Role of rainfall in the development of coffee berry disease in coffea arabica caused by colletotrichum kahawae, in cameroon, Plant pathology 59 (2) (2010) 324–329.

© 2025 NSP
Natural Sciences Publishing Cor.

[6] A. L. Gaitán, M. A. Cristancho, B. L. C. Caicedo, C. A. Rivillas, G. C. Gómez, Compendium of coffee diseases and pests, APS Press, The American Phytopathological Society, 2015.
[7] M. Silva, M. Nicole, L. Rijo, J. Geiger, C. Rodrigues, Jr, Cytochemical aspects of the plant–rust fungus interface during the compatible interaction coffea arabica (cv. caturra)–hemileia vastatrix (race iii), International Journal of Plant Sciences 160 (1) (1999) 79–91.
[8] K. Alemu, G. Adugna, F. Lemessa, D. Muleta, Current status of coffee berry disease (colletotrichum kahawae waller & bridge) in ethiopia, Archives of Phytopathology and Plant Protection 49 (17-18) (2016) 421–433.
[9] A. Girma, J. Chala, Resistance levels of arabica coffee cultivars to coffee berry disease, coffee wilt and leaf rust diseases in ethiopia, in: Proceedings of the 12th Conference of the Crop Science Society of Ethiopia (CSSE), 2008, pp. 92–103.
[10] E. GRIFFITHS, J. Gibbs, J. Waller, Control of coffee berry disease, Annals of applied biology 67 (1) (1971) 45–74.
[11] D. Fotsa, E. Houpa, D. Bekolle, C. Thron, M. Ndoumbe, Mathematical modelling and optimal control of anthracnose, arXiv preprint arXiv:1307.1754.
[12] J. Shi, D. Han, C. Chen, X. Shen, Ktmn: Knowledge-driven two-stage modulation network for visual question answering, Multimedia Systems 30 (6) (2024) 1–17.
[13] Q. Wang, X. Xiang, B. Chen, Food protein based nanotechnology: from delivery to sensing systems, Current Opinion in Food Science (2024) 101134.
[14] H. Gong, J. Sardans, H. Huang, Z. Yan, Z. Wang, J. Peñuelas, Global patterns and controlling factors of tree bark c: N: P stoichiometry in forest ecosystems consistent with biogeochemical niche hypothesis, New Phytologist.
[15] H. Jiang, S. M. Li, W. G. Wang, Moderate deviations for parameter estimation in the fractional ornstein-uhlenbeck processes with periodic mean, Acta Mathematica Sinica, English Series 40 (5) (2024) 1308–1324.
[16] Q. Chen, X. Mei, J. He, J. Yang, K. Liu, Y. Zhou, C. Ma, J. Liu, S. Zeng, L. Zhang, et al., Modeling and compensation of small-sample thermal error in precision machine tool spindles using spatial–temporal feature interaction fusion network, Advanced Engineering Informatics 62 (2024) 102741.
[17] X. Shi, U. Ishtiaq, M. Din, M. Akram, Fractals of interpolative kannan mappings, Fractal and Fractional 8 (8) (2024) 493.
[18] X. Pi, D. Yan, Y. Xu, M. Pan, Z. Wang, M. Chang, Z. Qi, Tlrs signaling pathway regulation, antibacterial and apoptotic activity of largemouth bass ecsit during edwardsiella piscicida infection, Aquaculture 595 (2025) 741615.
[19] S. Meng, F. Meng, F. Zhang, Q. Li, Y. Zhang, A. Zemouche, Observer design method for nonlinear generalized systems with nonlinear algebraic constraints with applications, Automatica 162 (2024) 111512.
[20] N. J. Cunniffe, C. A. Gilligan, Invasion, persistence and control in epidemic models for plant pathogens: the effect of host demography, Journal of the Royal Society Interface 7 (44) (2010) 439–451.
[21] Y. Fotso Fotso, S. Touzeau, B. Tsanou, S. Bowong, F. Grognard, Modelling and optimal strategy to control coffee berry borer, Mathematical Methods in the Applied Sciences 44 (18) (2021) 14569–14592.
[22] Y. Zhang, X. Wang, X. Wang, H. A. Mang, Virtual displacement based discontinuity layout optimization, International Journal for Numerical Methods in Engineering 123 (22) (2022) 5682–5694.
[23] Y. Zhang, M. Zeiml, C. Pichler, R. Lackner, Model-based risk assessment of concrete spalling in tunnel linings under fire loading, Engineering structures 77 (2014) 207–215.
[24] T. Abraha, F. Al Basir, L. L. Obsu, D. F. Torres, Pest control using farming awareness: Impact of time delays and optimal use of biopesticides, Chaos, Solitons & Fractals 146 (2021) 110869.
[25] D. J. F. Mbogne, C. Thron, Optimal control of anthracnose using mixed strategies, Mathematical Biosciences 269 (2015) 186–198.
[26] D. Zhang, L. G. Pee, S. L. Pan, J. Wang, Information practices in data analytics for supporting public health surveillance, Journal of the Association for Information Science and Technology 75 (1) (2024) 79–93.
[27] A. S. Melese, O. D. Makinde, L. L. Obsu, Mathematical modelling and analysis of coffee berry disease dynamics on a coffee farm, Mathematical Biosciences and Engineering 19 (7) (2022) 7349–7373.
[28] H. Nyaberi, W. Mutuku, D. Malonza, G. Gachigua, et al., A mathematical model of the dynamics of coffee berry disease, Journal of Applied Mathematics 2023.
[29] Z. Wu, C. Ma, L. Zhang, H. Gui, J. Liu, Z. Liu, Predicting and compensating for small-sample thermal information data in precision machine tools: A spatial-temporal interactive integration network and digital twin system approach, Applied Soft Computing 161 (2024) 111760.
[30] S. Bushnaq, K. Shah, H. Alrabaiah, On modeling of coronavirus-19 disease under mittag-leffler power law, Advances in Difference Equations 2020 (1) (2020) 487.
[31] R. Jan, M. A. Khan, P. Kumam, P. Thounthong, Modeling the transmission of dengue infection through fractional derivatives, Chaos, Solitons & Fractals 127 (2019) 189–216.
[32] W. Xu, E. Aponte, P. Vasanthakumar, The property ($\omega\pi$) as a generalization of the a-weyl theorem, Aims Math 9 (9) (2024) 25646–25658.

© 2025 NSP
Natural Sciences Publishing Cor.

[33] K. Diethelm, The analysis of fractional differential equations: an application-oriented exposition using differential operators of Caputo type, Vol. 2004, Springer Berlin, 2010.
[34] M. Caputo, M. Fabrizio, A new definition of fractional derivative without singular kernel, Progress in Fractional Differentiation & Applications 1 (2) (2015) 73–85.
[35] A. Atangana, Blind in a commutative world: simple illustrations with functions and chaotic attractors, Chaos, Solitons & Fractals 114 (2018) 347–363.
[36] E. Bonyah, J. Gomez-Aguilar, A. Adu, Stability analysis and optimal control of a fractional human african trypanosomiasis model, Chaos, Solitons & Fractals 117 (2018) 150–160.
[37] A. Atangana, D. Baleanu, New fractional derivatives with nonlocal and non-singular kernel: theory and application to heat transfer model, arXiv preprint arXiv:1602.03408.
[38] Y. Zhang, X. Zhuang, R. Lackner, Stability analysis of shotcrete supported crown of natm tunnels with discontinuity layout optimization, International Journal for Numerical and Analytical Methods in Geomechanics 42 (11) (2018) 1199–1216.
[39] N. Sweilam, S. Al-Mekhlafi, D. Baleanu, Optimal control for a fractional tuberculosis infection model including the impact of diabetes and resistant strains, Journal of advanced research 17 (2019) 125–137.
[40] Z. Huang, K. Li, Y. Jiang, Z. Jia, L. Lv, Y. Ma, Graph relearn network: Reducing performance variance and improving prediction accuracy of graph neural networks, Knowledge-Based Systems 301 (2024) 112311.
[41] Y. Zhang, Z. Gao, X. Wang, Q. Liu, Predicting the pore-pressure and temperature of fire-loaded concrete by a hybrid neural network, International Journal of Computational Methods 19 (08) (2022) 2142011.
[42] H. Singh, Analysis for fractional dynamics of ebola virus model, Chaos, Solitons & Fractals 138 (2020) 109992.
[43] H. Singh, Analysis of drug treatment of the fractional hiv infection model of cd4+ t-cells, Chaos, Solitons & Fractals 146 (2021) 110868.
[44] J. Huang, C. Feng, X. Wang, Y. Zhang, Continuous–discontinuous element method for simulating three-dimensional reinforced concrete structures, Structural Concrete.
[45] O. Balatif, L. Boujallal, A. Labzai, M. Rachik, Stability analysis of a fractional-order model for abstinence behavior of registration on the electoral lists, International Journal of Differential Equations 2020.
[46] E. Bonyah, A. Atangana, M. Chand, Analysis of 3d is-lm macroeconomic system model within the scope of fractional calculus, Chaos, Solitons & Fractals: X 2 (2019) 100007.
[47] M. A. Khan, A. Atangana, Modeling the dynamics of novel coronavirus (2019-ncov) with fractional derivative, Alexandria Engineering Journal 59 (4) (2020) 2379–2389.
[48] S. Okyere, J. A. Prah, M. O. Fokuo, A model of covid-19 with underlying health condition using fraction order derivative, arXiv preprint arXiv:2201.11659.
[49] T. Abdeljawad, D. Baleanu, Integration by parts and its applications of a new nonlocal fractional derivative with mittag-leffler nonsingular kernel, arXiv preprint arXiv:1607.00262.
[50] C. T. Deressa, G. F. Duressa, Analysis of atangana–baleanu fractional-order seair epidemic model with optimal control, Advances in Difference Equations 2021 (1) (2021) 1–25.
[51] S. K. Panda, Applying fixed point methods and fractional operators in the modelling of novel coronavirus 2019-ncov/sars-cov-2, Results in Physics 19 (2020) 103433.
[52] Z. M. Odibat, N. T. Shawagfeh, Generalized taylor's formula, Applied Mathematics and Computation 186 (1) (2007) 286–293.

© 2025 NSP
Natural Sciences Publishing Cor.